Direct Fabrication of Ferrite MFe_2O_4 (M = Zn, Mg)/Fe Composite Thin Films by Soft Solution Processing

Shu-Hong Yu† and Masahiro Yoshimura*

Center for Materials Design, Materials and Structures Laboratory, Tokyo Institute of Technology, 4259 Nagatsuta, Midori-ku, Yokohama 226-8503, Japan

Received August 28, 2000. Revised Manuscript Received October 17, 2000

Spinel ferrite/metal composite thin films of MFe_2O_4/Fe (M = Zn, Mg) with controlled grain sizes and shape were directly fabricated by a soft solution-processing route that involved the liquid−solid interfacial hydrothermal reaction of an Fe substrate with metal ions M^{2+} (M = Zn, Mg) in ammonia solution at lower temperatures (<200 °C). The grain particles of $ZnFe_2O_4$/Fe composite thin films show a well-developed octahedral shape with highly {111} preferential orientation, whereas the grain particles of $MgFe_2O_4$/Fe thin films displayed spherical shape. The saturation magnetization of the ferrite/Fe composites thin films was found to be much improved compared with that of single-phase ferrite products, and the ferrite/Fe thin films displayed superparamagnetism. The present soft-solution processing route will be extended to fabricate other novel ceramic/metal composite thin films.

Introduction

Ferrites are a group of technologically important materials that are used as magnetic recording materials, microwave devices, humidity sensors, and pigments, etc. Spinel ferrites, MFe_2O_4 (M = Mn, Co, Ni, Zn, Mg), are among the most important magnetic materials and have been widely used for electronic applications over the past half century.[1] Conventionally, spinel ferrite particles can be prepared by solid-state, evaporative decomposition of solutions (EDS), hydrolysis of metal organics, decomposition of metal organic solution, solid-solution precursor, and wet methods.[2−6]

In recent years, various methods have been developed for the synthesis of ferrite nanomaterials, such as self-propagating high-temperature synthesis of ferrites MFe_2O_4(M = Mg, Ba, Co, Ni, Cu, Zn) from metal oxides or peroxides in an external magnetic field at high temperatures (950−1050 °C),[7] a new solid-state exchange reaction of lithium ferrites with $ZnSO_4$ in air at 650−750 °C for producing $ZnFe_2O_4$ powders,[8] a ball-milling technique for producing $ZnFe_2O_4$ and $MgFe_2O_4$ nanoparticles,[9] and coprecipitation reaction.[10] Some other emerging preparation methods in recent years include sonochemical reactions,[11] gel−sol,[12] and micelles.[13]

Especially because the available hard magnetic materials have a lower saturation magnetization than many soft magnetic materials, researchers turn their attention to the use of composite materials. Therefore, ceramic/metal nanocomposites[14−17] and composites thin films[18−21] have attracted much attention because of their unique mechanical, electrical, and magnetic properties. Metal/$CoFe_2O_4$ thin films were prepared by a reactive sputtering method at 400 °C to improve the saturation magnetization (M_s).[21] Both a hydrothermal method and microwave-hydrothermal method were

* To whom correspondence should be addressed. E-mail: yoshimu1@rlem.titech.ac.jp. Tel.: +81 45 924 5323. Fax: +81 45 924 5358.
† E-mail: shyu1@rlem.titech.ac.jp.

(1) Sugimoto, M. *J. Am. Ceram. Soc.* **1999**, *82*, 269.
(2) Oda, K.; Yoshio, T.; Hirata, K.; O-oka, K.; Takahashi, K. *J. Jpn. Soc. Powder Metall.* **1982**, *29* (5), 170.
(3) Suwa, Y.; Hirano, S.; Itozawa, K.; Naka, S. In *Ferrites*: *Proceedings of the International Conference*, Tokyo, Japan, 1980; pp 23−26 .
(4) Higuchi, K.; Naka, S.; Hirano, S. *Adv. Ceram. Mater.* **1986**, *1*(1), 104.
(5) Komarneni, S.; Sankar, S. G. Metal Organic Solution Route to Synthesize Ferrites for Microwave Applications. In *88th Annual Meeting Abstracts*; American Ceramic Society, Columbus, OH, 1986; p 258.
(6) Ravindranathan, P.; Patil, K. C. *Am. Ceram. Soc. Bull.* **1987**, *66* (4), 688.
(7) Cross, W. B.; Affleck, L.; Kuznetsov, M. V.; Parkin, I. P.; Pankurst, Q. A. *J. Mater. Chem.* **1999**, *9*, 2524.
(8) Shlyakhtin, O. A.; Vjunitsky, I. N.; Oh, Y. J.; Tretyakov, Y. D. *J. Mater. Chem.* **1999**, *9*, 1223.
(9) Goya, G. F.; Rechenberg, H. R. *J. Magn. Magn. Mater.* **1999**, *203*, 141. Fatemi, D. J.; Harris, V. G.; Browning, V. M.; Kirkland, J. P. *J. Appl. Phys.* **1998**, *83*, 6867. Moustafa, S. F.; Morsi, M. B. *Mater. Lett.* **1998**, *34*, 241.
(10) Sato, T.; Haneda, K.; Seki, M.; Iijima, T. *Appl. Phys. A* **1988**, *50*, 13. Seki, M.; Sato, T.; Usui, S. *J. Appl. Phys.* **1988**, *63*, 1424. Chen, Q.; Rondinone, A. J.; Chakkoumakos, B. C.; Zhang, Z. J. *J. Magn. Magn. Mater.* **1999**, *194*, 1.
(11) Shafi, K. V. P. M.; Koltypin, Y.; Gedanken, A.; Prozorov, R.; Balogh, J.; Lendvai, J.; Felner, I. *J. Phys. Chem. B* **1997**, *101*, 6409.
(12) Sugimoto, T.; Shimotsuma, Y.; Itoh, H. *Powder Technol.* **1998**, *96*, 85.
(13) Feltin, N.; Pileni, M. P. *Langmuir* **1996**, *13*, 3927. Hochepied, J. F.; Bonville, P.; Pileni, M. P. *J. Phys. Chem. B* **2000**, *104*, 905. Liu, C.; Zou, B. S.; Rondinone, A. J.; Zhang, Z. J. *J. Phys. Chem.* **2000**, *104* (6), 1141.
(14) Ding, J.; Miao, W. F.; Street, R.; McCormick, P. G. *Script Mater.* **1996**, *35* (11), 1307.
(15) Pourroy, G. *J. Alloy. Compd.* **1998**, *278*, 264.
(16) Bercoff, P. G.; Bertorello, H. R. *J. Magn. Magn. Mater.* **1998**, *187*, 169.
(17) Bercoff, P. G.; Bertorello, H. R. *J. Magn. Magn. Mater.* **1999**, *205*, 261.
(18) Han, S. H.; Han, S. M.; Kim, H. J.; Kang, I. K. *IEEE Trans.* **1996**, *MAG-32*, 4499.
(19) Hiratsuka, N.; Kaodoshima, T.; Fujita, M.; Sugimoto, M. *J. Powder. Powder Met. Jpn.* **1992**, *39*, 989.
(20) Na, J. G.; Kim, C. S. *IEEE Trans.* **1996**, *MAG-32*, 3611.
(21) Na, J. G.; Park, C. H.; Park, K.; Lee, S. R. *Mater. Res. Bull.* **1997**, *32* (10), 1395.

10.1021/cm000691y CCC: $19.00
Published on Web 11/23/2000

developed for the synthesis of ferrites powders.[22,23] A method called the ferrite-plating technique in aqueous solution was reported for preparing ferrite thin films.[24]

Soft solution processing (SSP) has proved to be a promising method for fabrication, shaping, sizing, and orientation of various oxide ceramics in aqueous solution via a one step without excess energy for firing, sintering, or melting.[25,26] In this article, spinel ferrite/metal composite thin films of MFe_2O_4/Fe (M = Zn, Mg) with controlled grain sizes and shape were directly fabricated by a one-step soft solution processing route at lower temperatures (<200 °C). The magnetic properties of the prepared composite thin films were investigated.

Experimental Section

MFe_2O_4 thin films were fabricated on an Fe substrate by interfacial hydrothermal reaction of an Fe substrate with metal ions M^{2+}(M = Zn, Mg) using ammonia solution in commercial stainless Teflon-lined autoclaves of 40-mL capacity (SANPLATEC Co., Japan). Reagent-grade $ZnCl_2$, $Mg(NO_3)_2 \cdot 6H_2O$, and ammonia solution (29% w/w, 15.3 M) (Wako Pure Chemical Industries, Ltd., Osaka, Japan) were used as reactants. Fe plates with 99.9% purity (Nilaco Co.) and dimensions of 1 × 5 × 10 mm were degreased in acetone with an ultrasonic cleaner, then ultrasonically cleaned with deionized water, and dried before hydrothermal reaction. The ammonia solution was used as received and its concentration was adjusted by adding different volume ratios of deionized water. In a typical preparation procedure, the Fe substrate was fixed at the bottom of the Teflon liner. Thirty milliliters of 0.1 M Zn^{2+} ammonia solution was prepared by dissolving 1.0×10^{-3} mol of $ZnCl_2$ in 30 mL of 29% ammonia solution, which was poured into the Teflon liner and sealed. The autoclave was maintained at 180 °C for 12 h and air cooled to room temperature. Then, the substrate was taken out from the solution, washed with deionized water, and dried for characterization. The products were characterized by X-ray powder diffraction (XRD) patterns employing a scanning rate of 0.02° s^{-1} in the 2θ range from 10° to 70°, using a MAC Science MXP-3VA diffractometer equipped with a graphite monochromatized Cu Kα radiation (λ = 1.5405 Å) operated at 40 mA and 40 kV. The scanning electron microcope (SEM) images of the films were obtained using a Hitachi SEM S-4500. The magnetic measurements were carried out with a superconducting quantum interference device (SQUID) magnetometer (Quantum Design MPMS-5s).

Results and Discussion

After hydrothermal reaction, well-crystallized $ZnFe_2O_4$ and $MgFe_2O_4$ thin films formed on the Fe substrates with medium brown black to deep brown color, which were confirmed by XRD patterns to be single phase with cubic spinel structure. The concentrations of M^{2+} (M = Zn, Mg) and ammonia solution, temperature, and reaction time on the formation, crystallinity, and microstructure of the thin films were investigated.

Figure 1 shows XRD patterns of $ZnFe_2O_4$ thin films formed on an Fe substrate in 29% ammonia solution (15.3 M) using different initial concentrations [Zn^{2+}]. Figure 1a showed that the crystallized $ZnFe_2O_4$ thin films did not form if the initial concentration [Zn^{2+}] is as low as 0.01 M at 180 °C for 12 h. Well-crystallized $ZnFe_2O_4$ thin films can be produced if [Zn^{2+}] was in the range of 0.025−0.5 M as shown in Figure 1b−g. A higher concentration of Zn^{2+} in the solution is more favorable for the crystallization of the thin films. Furthermore, the concentration of ammonia solution also played an important role in the films' formation, grain sizes, and microstructures.

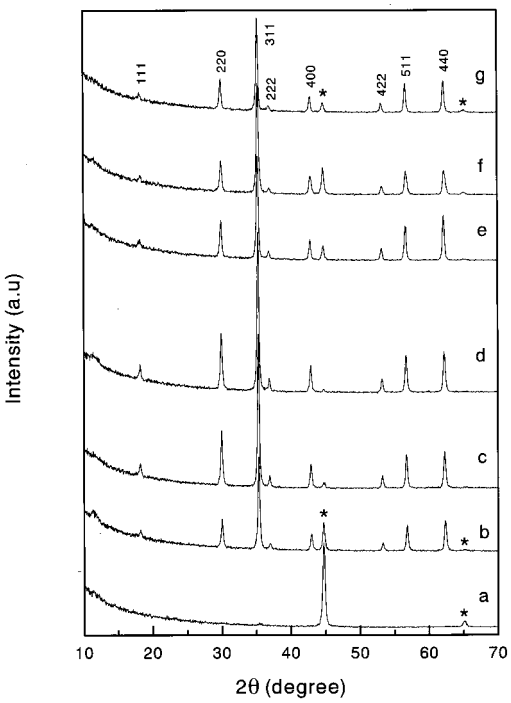

Figure 1. XRD patterns for as-prepared $ZnFe_2O_4$/Fe composite films in 29% ammonia solution (15.3 M) at 180 °C for 12 h under different concentrations of Zn^{2+}: (a) [Zn^{2+}] = 0.01 M; (b) [Zn^{2+}] = 0.025 M; (c) [Zn^{2+}] = 0.05 M; (d) [Zn^{2+}] = 0.1 M; (e) [Zn^{2+}] = 0.2 M; (f) [Zn^{2+}] = 0.3 M; (g) [Zn^{2+}] = 0.5 M. Fe substrate (*).

If the ammonia solution was diluted to as low as 3:1 (29% ammonia solution/H_2O, v/v, 11.5 M) or the reaction time was lower than 4 h, $ZnFe_2O_4$ thin films were found to be poorly crystallized. While the temperature was lower than 140 °C, the films were not produced. In contrast, $MgFe_2O_4$ thin films are more easily produced, using even a lower concentration of Mg^{2+}, or more diluted ammonia solution, or lower temperatures. Figure 2 shows the XRD patterns for $MgFe_2O_4$ thin films produced in various concentrations of ammonia solution. Well-crystallized $MgFe_2O_4$ thin films can be produced in 0.01 M Mg^{2+} ammonia solution (29% w/w, 15.3 M). In addition, crystallized $MgFe_2O_4$ thin films can also be produced in diluted ammonia solution, which was as low as 1:1 (29% ammonia solution/H_2O, v/v, 7.6 M) at 180 °C for 12 h. The results demonstrate that the thin films obtained at a higher concentration of ammonia solution have better crystallinity than those obtained at a lower concentration of ammonia solution, as shown in Figure 2.

The formation diagram of MFe_2O_4 thin films as a function of initial concentration of [M^{2+}] (M = Zn, Mg) and ammonia concentration was shown in Figure 3.

SEM was taken to examine the morphologies and particle sizes of the thin films. $ZnFe_2O_4$ thin films

(22) Komarneni, S.; Fregeau, E.; Breval, E.; Roy, R. *J. Am. Ceram. Soc.* **1988**, *71* (1), C-26.
(23) Komarneni, S.; D'Arrigo, M. C.; Leonelli, C.; Pellacani, G. C.; Katsuki, H. *J. Am. Ceram. Soc.* **1998**, *81* (11), 3041.
(24) Abe, M.; Tamaura, Y. *Jpn. J. Appl. Phys.* **1983**, *22*, L551.
(25) Yoshimura, M. *J. Mater. Res.* **1998**, *13*, 796. Yoshimura, M.; Sunchanek, W. *Solid State Ionics* **1997**, *98*, 197. Yoshimura, M.; Sunchanek, W.; Han, K.-S. *J. Mater. Chem.* **1999**, *9*, 77.
(26) Yoshimura, M.; Sunchanek, W.; Byrappa, K. *Mater. Res. Soc. Bull.* **2000**, *35* (9), 17.

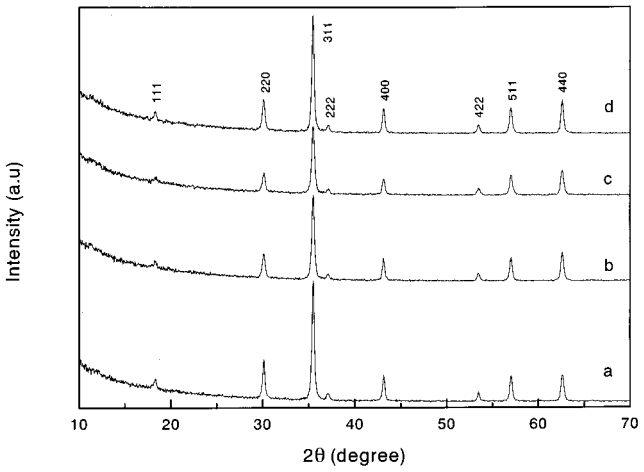

Figure 2. XRD patterns for as-prepared $MgFe_2O_4$/Fe composite films in different ammonia concentration solutions at 180 °C for 12 h, $[Mg^{2+}] = 0.1$ M: (a)−(c), 29% ammonia solution/H_2O (v/v) = 1:1, 2:1, and 5:1 (7.6, 10.2, and 12.8 M, respectively); (d) 29% ammonia solution (15.3 M). Fe substrate (*).

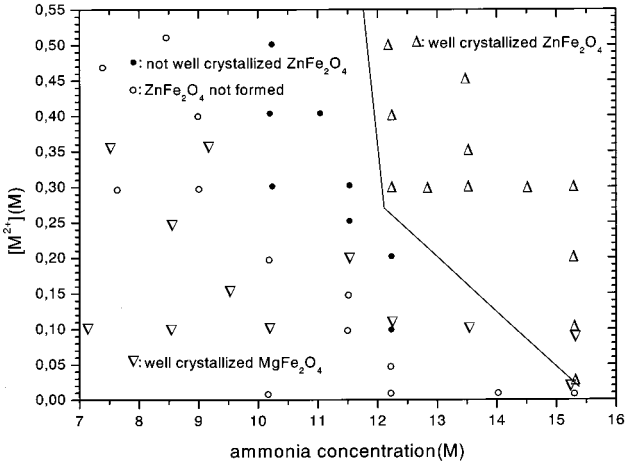

Figure 3. Formation diagram of MFe_2O_4 (M = Zn, Mg) thin films as a function of $[M^{2+}]$ concentration and ammonia concentration.

produced in higher Zn^{2+} concentration solution consisted of well-developed octahedral shape $ZnFe_2O_4$ grain particles with a uniform size of 2.3 μm as shown in Figure 4a, which is caused by {111} preferential orientation crystal growth. Figure 4a−d shows the influence of $[Zn^{2+}]$ on the grain sizes and shape of the thin films, which demonstrated that the grain size can be controlled in the range of 0.3−2.3 μm by changing $[Zn^{2+}]$ from 0.025 to 0.5 M. Figure 4g−i showed that $MgFe_2O_4$ thin films obtained at 180 °C for 12 h consist of uniform, spherical particles with different sizes in the range of 65−130 nm by varying the initial Mg^{2+} concentration. The results suggested that grain sizes and shape of the ferrite thin films were well controlled by changing the reaction conditions.

The possible reactions for the formation of MFe_2O_4 (M = Zn, Mg) in the present system can be expressed as in eqs 1−9. According to the Pourbaix diagram, [27] metal Fe reacted with H_2O to form $Fe(OH)_2$ and further was oxidized to be $[Fe(OH)_n]^{-(n-3)}$ ($n = 2, 3$) by the small amount of dissolved O_2 in solution as shown in eqs 1 and 2. In addition, the metal ions Zn^{2+} will form different soluble Zn species as shown in eqs 3−7 due to the amphoteric property of $Zn^{2+}$and strong coordinating ability with NH_3. When Mg^{2+} is presented in ammonia solution, $Mg(OH)_2$ will form quickly as shown in eq 8. Finally, soluble Zn species and newly formed $Mg(OH)_2$ will react with hydroxy complexes $[Fe(OH)_n]^{-(n-3)}$ to form spinel MFe_2O_4. Here, the newly formed $Mg(OH)_2$ plays a key role in the formation of the $MgFe_2O_4$ phase because no spinel phase formed if commercial $Mg(OH)_2$ was used instead of $Mg(NO_3)_2 \cdot 6H_2O$ as the reactant. We attribute it to the very poor solubility of commercial $Mg(OH)_2$ in ammonia solution. The formation mecha-

$$Fe + 2H_2O \rightarrow Fe(OH)_2 + H_2 \quad (1)$$

$$Fe(OH)_2 + OH^- + O_2 + H_2O \rightarrow [Fe(OH)_n]^{-(n-3)} \quad (n = 2, 3) \quad (2)$$

$$Zn^{2+} + H_2O \leftrightarrow ZnOH^+ + H^+ \quad (3)$$

$$ZnOH^+ + H_2O \leftrightarrow HZnO_2^- + 2H^+ \quad (4)$$

$$Zn^{2+} + 2H_2O \leftrightarrow HZnO_2^- + 3H^+ \quad (5)$$

$$HZnO_2^- \leftrightarrow ZnO_2^{2-} + H^+ \quad (6)$$

$$Zn^{2+} + n NH_3 \cdot H_2O \leftrightarrow Zn(NH_3)_n^{2+} + nH_2O \quad (n = 1-4) \quad (7)$$

$$Mg^{2+} + 2OH^- \rightarrow Mg(OH)_2 \quad (8)$$

$$\text{soluble M species} + [Fe(OH)_n]^{-(n-3)} \rightarrow MFe_2O_4 \quad (M = Zn, Mg) \quad (9)$$

nism of the ferrite thin films may involve multiple reaction mechanisms,[28] for example, in situ transformation mechanism[29] and dissolution−precipitation mechanism,[30] which were proposed for explaining the hydrothermal formation of $BaTiO_3$. In the in situ transformation mechanism, the dissolved $[Fe(OH)_n]^{-(n-3)}$ reacts initially with dissolved M species (M = Zn, Mg) followed by supersaturation and produces a continuous layer of MFe_2O_4 on an Fe substrate through which the additional M species and Fe species must diffuse for reaction (9) to continue, until their supply is completely exhausted. Two possible rate-controlling processes may exist, that is, the diffusion of the M species and Fe species through the spinel layer and the reaction between the M species and $[Fe(OH)_n]^{-(n-3)}$. In the dissolution−precipitation mechanism, produced dissolved $[Fe(OH)_n]^{-(n-3)}$ species react with M species in solution to precipitate MFe_2O_4 on an Fe substrate possibly by either heterogeneous nucleation or homogeneous nucleation in bulk solution. Rapid dissolution

(27) Pourbaix, M. *Atlas of Electrochemical Equilibria in Aqueous Solution*, 2nd ed.; National Association of Corrosion Engineers: Houston, TX, 1974; pp 313, 409, 141,

(28) Eckert, J. O. E., Jr.; Huang-Houston, C. C.; Gersten, B. L.; Lencka, M. M.; Riman, R. E. *J. Am. Ceram. Soc.* **1996**, *79* (11), 2929.
(29) Hertl, W. *J. Am. Ceram. Soc.* **1988**, *71*, 879.
(30) Ovramenko, N. A.; Shvets, L. I.; Ovcharenko, F. D.; Kornilovich, B. Y. *Izv. Akad. Nauk SSSR, Neorg. Mater.* **1979**, *15*, 1182.

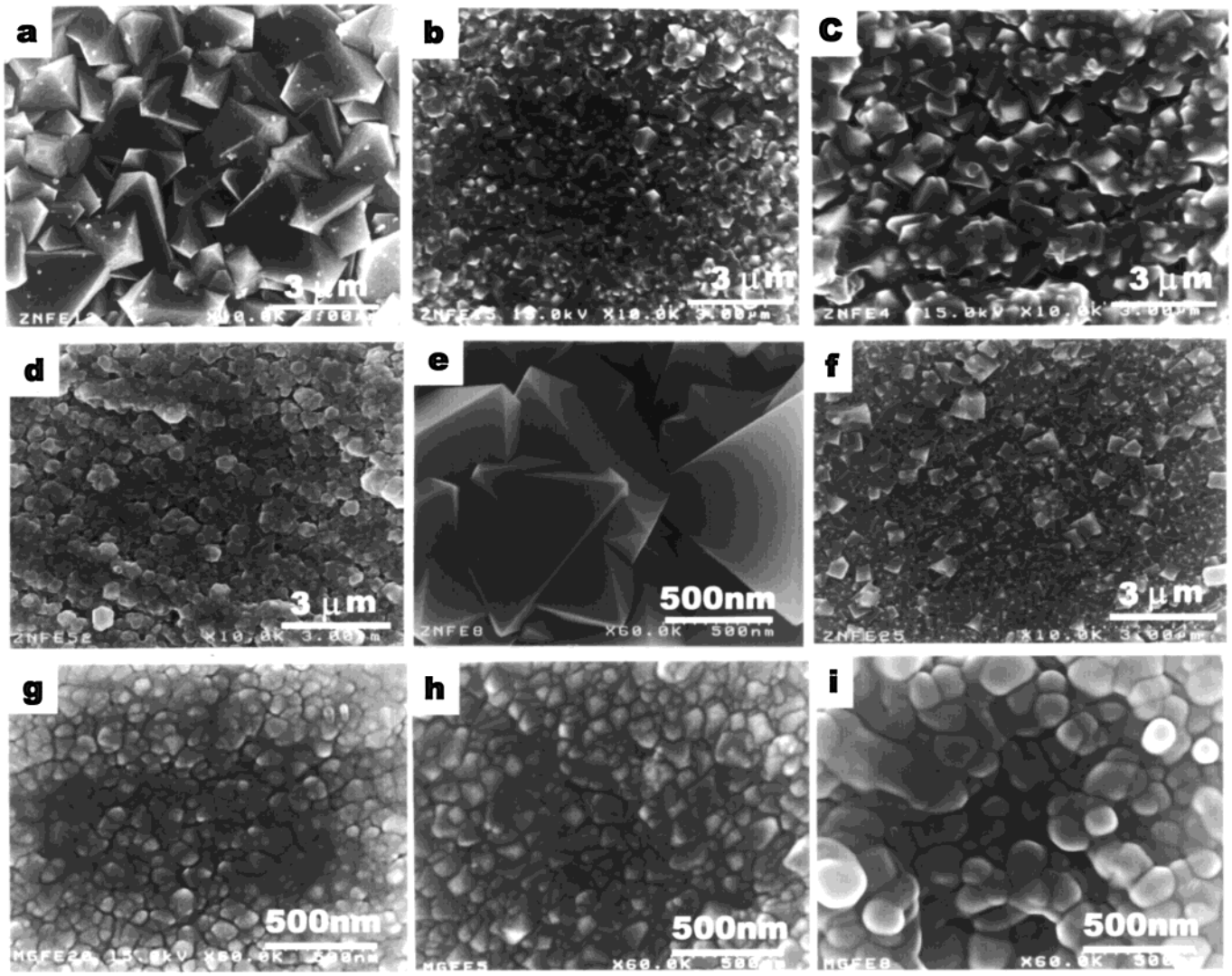

Figure 4. SEM images for as-prepared $ZnFe_2O_4$/Fe and $MgFe_2O_4$/Fe composite films in ammonia solution under different conditions. (a)−(f) $ZnFe_2O_4$/Fe: (a)−(d) 180 °C, 12 h, 29% ammonia solution (15.3 M), $[Zn^{2+}] = 0.5$, 0.3, 0.1, and 0.025 M, respectively; (e) 180 °C, 12 h, 29% ammonia solution/H_2O (v/v) = 5:1 (12.8 M), $[Zn^{2+}] = 0.1$ M; (f) 140 °C, 12 h, 29% ammonia solution, $[Zn^{2+}] = 0.1$ M. (g)−(i) $MgFe_2O_4$/Fe: 180 °C, 12 h, 29% ammonia solution (15.3 M), $[Mg^{2+}] = 0.3$, 0.025, and 0.01 M, respectively.

of Fe species from an Fe substrate provides the solution with a sufficient supply of Fe species, whereas slow dissolution starves the solution of reactant species, therefore, decreasing the reaction rate. The formation of a continuous MFe_2O_4 layer will reduce the supply of the Fe species and halt the rate of the formation of MFe_2O_4 via a dissolution−precipitation mechanism. In fact, these two mechanisms may compete for rate control in the present reaction system.

The interesting grain size dependence of MFe_2O_4 thin films on the initial concentration $[M^{2+}]$ was shown in Figure 5, which may be due to different rate-controlling steps involved in the formation of MFe_2O_4 thin films. Figure 5a shows that the grain size of $ZnFe_2O_4$ thin films increased from 0.3 to 0.9 μm with increasing $[Zn^{2+}]$ from 0.025 to 0.1 M. It is interesting that further increasing of $[Zn^{2+}]$ up to 0.3 M will lead to the decreasing of grain size to 0.4 μm. Then, the grain size again increased up to 2.3 μm with increasing $[Zn^{2+}]$ up to 0.5 M. In contrast, the grain size of $MgFe_2O_4$ thin films decreased with increasing initial concentration $[Mg^{2+}]$ as shown in Figure 5b. We believe that two possible mechanisms may act and compete for rate

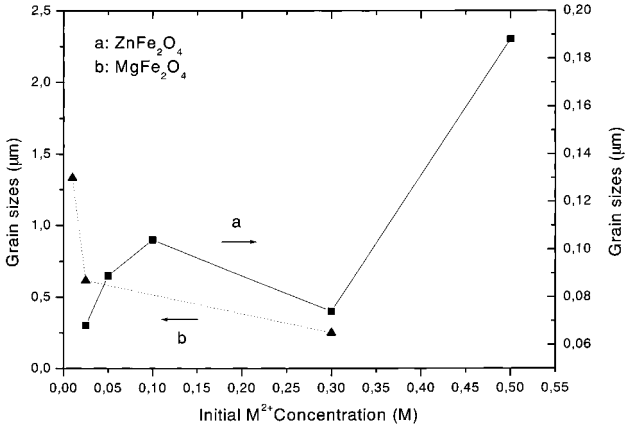

Figure 5. Grain size dependence on the initial M^{2+} concentration for as-prepared $ZnFe_2O_4$/Fe and $MgFe_2O_4$/Fe composite films produced at 180 °C for 12 h in 29% ammonia solution (15.3 M).

control in present reaction systems, which cause the grain sizes dependence on the initial $[M^{2+}]$.

Above the grain size dependence on the initial $[Zn^{2+}]$ could be explained as follows: (i) When $[Zn^{2+}]$ was in

the range of 0.025−0.1 M, the pH value of solution was higher (pH = 13.0−13.3) and not much changed as increasing $[Zn^{2+}]$, which was not favorable for the formation of dissolved Fe species and has no larger influence on the concentration of dissolved Fe species and the solubility of $ZnFe_2O_4$. Two possible mechanisms may act in this stage. In the beginning, the dissolution−precipitation mechanism will dominate. Zn species in the solution are not enough for supersaturation of the solution; increasing initial $[Zn^{2+}]$ will be favorable for accelerating the growth rate compared with the nucleation rate; therefore, the grain sizes increase. In addition, the slow dissolution of Fe species from an Fe substrate will starve the solution of reactant species and lead to the decrease of reaction rate and the increase of growth rate. With prolonged time a continuous $ZnFe_2O_4$ layer formed on an Fe substrate, and then the in situ transformation mechanism could be dominant. Increasing $[Zn^{2+}]$ will increase the diffusional rate of the Zn species through the ferrite layer; however, the concentration of dissolved Fe species is much lower compared with that of the Zn species. Therefore, increasing $[Zn^{2+}]$ will also accelerate the growth rate of $ZnFe_2O_4$ and lead to the increase of the grain size. (ii) Further increasing $[Zn^{2+}]$ from 0.1 to 0.3 M will result in the drop of the pH value of the solution to 12.7, and it will be more favorable for increasing dissolved Fe species in the solution. The dissolution−precipitation mechanism may dominate in this stage. The larger increase of Fe species in solution will increase the nucleation rate and lead to the decrease of the grain sizes. In addition, the drop in pH will increase the supersaturation of the solution due to the possible decrease of solubility of $ZnFe_2O_4$, which will increase the nucleation rate and also decrease the sizes. (iii) When increasing $[Zn^{2+}]$ from 0.3 to 0.5 M, the pH value of the solution changed from 12.7 to 12.5. This stage would be similar to that in the first case (i); the pH value does not have a larger influence on the dissolved Fe species and the solubility of $ZnFe_2O_4$ in the solution. Both mechanisms may compete for rate control in this stage. Again, the concentration of Zn species is relatively higher than that of the Fe species. The increase of Zn species will be favorable for accelerating the growth rate compared with the nucleation rate, therefore, leading to increasing grain sizes. In contrast, the relatively slow dissolution of Fe species from an Fe substrate will lead to the decrease of reaction rate and the increase of growth rate. With prolonged time, the in situ transformation mechanism could be dominant. Increasing $[Zn^{2+}]$ will also accelerate the growth rate of $ZnFe_2O_4$ due to the fact that the concentration of dissolved Fe species is much lower than that of the Zn species; therefore, the grain size will increase.

In the case of $MgFe_2O_4$ thin films, fresh white $Mg(OH)_2$ will precipitate while Mg^{2+} is added into ammonia solution. Because of the poor solubility of $Mg(OH)_2$ in alkaline solution, the solution has been supersaturated. When the initial $[Mg^{2+}]$ is increased from 0.01 to 0.3 M, the pH value of the solution will drop sharply from 13.1 to 11.6. Therefore, it will be more favorable to increase the dissolved Fe species in solution and increase the supersaturation of the solution because of the possible decrease of solubility of $MgFe_2O_4$, providing a larger amount of nuclei and increasing the nucleation rate, which will lead to decreasing grain sizes. Similar to the case of $ZnFe_2O_4$, both mechanisms may act and compete for rate control.

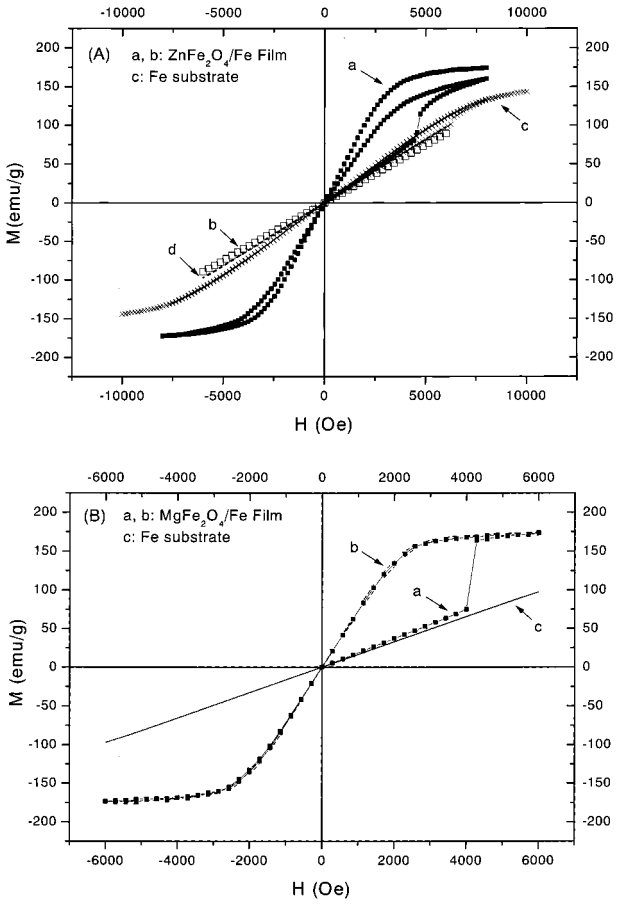

Figure 6. Magnetization vs applied magnetic field for MFe_2O_4/Fe composite films and bear Fe substrate. (A) $ZnFe_2O_4$/Fe composite films: (a) Zn^{2+} = 0.3 M, 180 °C, 12 h, 5 K (■); (b) $[Zn^{2+}]$ = 0.3 M, 180 °C, 12 h, 300 K (□); (c) $[Zn^{2+}]$ = 0.5 M, 180 °C, 12 h, 5 K (×); (d) bare Fe substrate (- - -). (B) $MgFe_2O_4$/Fe composite films: (a) $[Mg^{2+}]$ = 0.025 M, 180 °C, 12 h, 300 K (■); (b) $[Mg^{2+}]$ = 0.025 M, 180 °C, 12 h, 80 K (- - -); (c) bare Fe substrate, 300 K (—).

In addition, increasing the ammonia concentration under constant $[Zn^{2+}]$ (or $[Mg^{2+}]$) concentration will decrease the supersaturation of the solution due to the possible increase of solubility of $ZnFe_2O_4$ (or $MgFe_2O_4$) and decrease the dissolved Fe species in solution, which will decrease the nucleation rate and thus increase the sizes. Figure 4c,e shows that the grain sizes decreased from 0.9 to 0.6 μm when the 29% ammonia solution (15.3 M) was changed to 5:1 ammonia solution (29% ammonia solution/H_2O, v/v, 12.8 M). In addition, $ZnFe_2O_4$ thin films obtained in the 5:1 ammonia solution (12.8 M) consisted of very uniform octahedral particles with smooth grain surfaces and uniform sizes of about 0.6 μm and displayed similar {111} preferential orientation growth as found in the 29% ammonia solution, indicating that the grain surfaces of the $ZnFe_2O_4$ particles obtained in a higher concentration ammonia solution were rougher than those in a lower concentration ammonia solution, which could also be caused by increasing solubility of $ZnFe_2O_4$ in the higher ammonia concentration solution under hydrothermal conditions.

Figure 6 shows the typical field dependence of the magnetization for the composite films and bare Fe

substrate. Figure 6A(a),(b) shows the magnetization curves taken at 5 and 300 K for as-prepared $ZnFe_2O_4$/Fe composite thin films. Rather large magnetization at 5 K for $ZnFe_2O_4$/Fe composite thin films with an average grain size of 0.9 μm (the sample in Figure 4c) has been observed as shown in Figure 6A(a) with saturation magnetization up to 172.3 emu/g, which is much higher than that reported for the single-phase $ZnFe_2O_4$ material in the literature.[31] The magnetization is similar to the bare Fe substrate when the applied magnetic field increased from 0 to 4570 Oe. Interestingly, when the applied magnetic field was increased further, a sharper jump occurred at 4573.4 Oe and the magnetization increased to 114.4 emu/g and slowly increased to saturation up to 172.3 emu/g while the magnetic field increased to 8000 Oe. It can be explained as being due to the antiferromagnetic characteristics of $ZnFe_2O_4$ ferrite thin films when the temperature is lower than the Néel temperature for bulk $ZnFe_2O_4$ ($T_N = 10$ K). Figure 6A(c) shows no hysteresis and nonlinear M versus H were observed at 5 K for $ZnFe_2O_4$/Fe thin films with larger grain sizes of 2.3 μm (sample in Figure 4a), which has a saturation magnetization of about 160.3 emu/g. However, no magnetic hysteresis was observed at 80 and 300 K, and M varies linearly with H as expected for paramagnetic materials. These magnetic characteristics are the same as those of the bare Fe substrate, which is a well-known ferromagnetic material with a Curie temperature of $T_c = 1043$ K ($M_s = 21\,980$ Oe). A nonlinear M versus H in the magnetic curves obviously indicated the absence of a purely paramagnetic phase. In addition, no hysteresis or remanence is observed in the data; therefore, the possibility of a long-range ferromagnetic or ferromagnetic order could be ruled out.[32] However, a nonlinear M versus H and the absence of hysteresis are expected characteristics for superparamagnetic particles presented in the thin films. Furthermore, the loops are symmetric about $H = 0$, which provides additional evidence for the presence of superparamagnetic grain particles in the films.[32] As prepared $MgFe_2O_4$/Fe composite thin films also clearly displayed superparamagnetic characteristics as shown in Figure 6B(a),(b). No hysteresis was observed for $MgFe_2O_4$/Fe composite thin films and they displayed paramagnetic magnetization both at 80 and 300 K with saturation magnetization up to 173.8 emu/g. The magnetization is similar to the bare Fe substrate when the applied magnetic field increased from 0 to 4000 Oe. Similarly, when the applied magnetic field was increased further, a sharper jump occurred at 4285 Oe and the magnetization increased to 164.2 emu/g and then slowly up to saturation to 6000 Oe. Although the superparamagnetism about single-phase MFe_2O_4 (M = Zn, Mg) films or nanoparticles has been reported,[32−34] the detailed magnetization mechanism for as-prepared ferrites/Fe composite thin films seems to be more complicated. Further investigations are still in progress.

Conclusions

We demonstrated a novel soft solution processing route for direct fabrication spinel ferrite/metal composite thin films of MFe_2O_4/Fe (M = Zn, Mg) with controlled grain sizes and shapes by using liquid−solid interfacial hydrothermal reaction of an Fe substrate with metal ions M^{2+} (M = Zn, Mg) in ammonia solution at lower temperatures (<200 °C). Both the grain sizes and shape were well controlled. The present soft solution processing route will be extended to fabricate other novel ceramic/metal composite thin films. Especially the magnetic properties of the ferrite/Fe composites thin films were found to be much improved compared with that of single-phase ferrite products and the films displayed unusual superparamagnetic characteristics. These kinds of ferrite/metal composite thin films may have unique mechanical, electrical, and magnetic properties and could have some potential applications in industries.

Acknowledgment. This work has been supported by the "Research for the Future Program" (No. 96R06901) of the Japan Society for Promotion of Science (JSPS).

CM000691Y

(31) Cross, W. B.; Affleck, L.; Kuznetsov, M. V.; Parkin, I. P.; Pankurst, Q. A. *J. Mater. Chem.* **1999**, *9*, 2524.
(32) Chen, J.; Srinvasan, G.; Hunter, S.; Babu, V. S.; Seehra, M. S. *J. Magn. Magn. Mater.* **1995**, *146*, 291.
(33) Chen, Q.; Zhang, Z. J. *Appl. Phys. Lett.* **1998**, *73* (21), 3156.
(34) Chen, Q.; Rondinone, A. J.; Chakkoumakos, B. C.; Zhang, Z. J. *J. Magn. Magn. Mater.* **1999**, *194*, 1.